Supplemental information for neonSoilFlux:

An R Package for Continuous Sensor-Based

Estimation of Soil CO₂ Fluxes

- John Zobitz¹ Ed Ayres² Zoey Werbin³ Ridwan Abdi¹
- Natalie Ashburner-Wright⁴ Lillian Brown⁴
- 6 Ryan Frink-Sobierajski⁴ Lajntxiag Lee¹ Dijonë Mehmeti¹
- ⁷ Christina Tran⁴ Ly Xiong¹ Naupaka Zimmerman^{4,5}

3

 $_{8}\quad ^{1}$ Augsburg University, 2211 Riverside Avenue, Minneapolis, MN 55454

⁹ National Ecological Observatory Network, Battelle, 1685–38th Street, Suite 100, Boulder,

¹⁰ CO 80301

 $^{^{\}rm 11}$ Boston University, 5 Cummington Street, Boston, MA 02215

 $^{^{\}rm 4}$ University of San Francisco, 2130 Fulton Street, San Francisco, CA 94117

 $^{^{\}rm 5}$ University of Kansas, 1251 Wescoe Dr. Lawrence, KS 66045

4 1 Assessment of data gaps

For a given half-hourly time period, the neonSoilFlux packages assigns a QA flag for a 15 measurement if more one values across all measurement depths uses gap-filled data (Section 16 4.2.1 of the main text). Panel a of Figure S1 reports the proportion of gap-filled data for all 17 input environmental measurements at each site during the period when field measurements 18 were made. Soil fluxes are computed from 4 different types of input measurements $(T_S, SWC,$ 19 P, and CO_2), any of which could have a QA flag in a half-hourly interval. Panel b of Figure S1 20 displays at each site the distribution of the number of different gap-filled measurements used 21 to compute a half-hourly flux. The largest cause of measurements needing to be gap-filled 22 was missing or flagged soil moisture data. Calculating fluxes for WOOD and SJER required 23 using the largest proportion of gap-filled measurements, due to substantially large fractions of 24 flagged or missing SWC and T_S data.

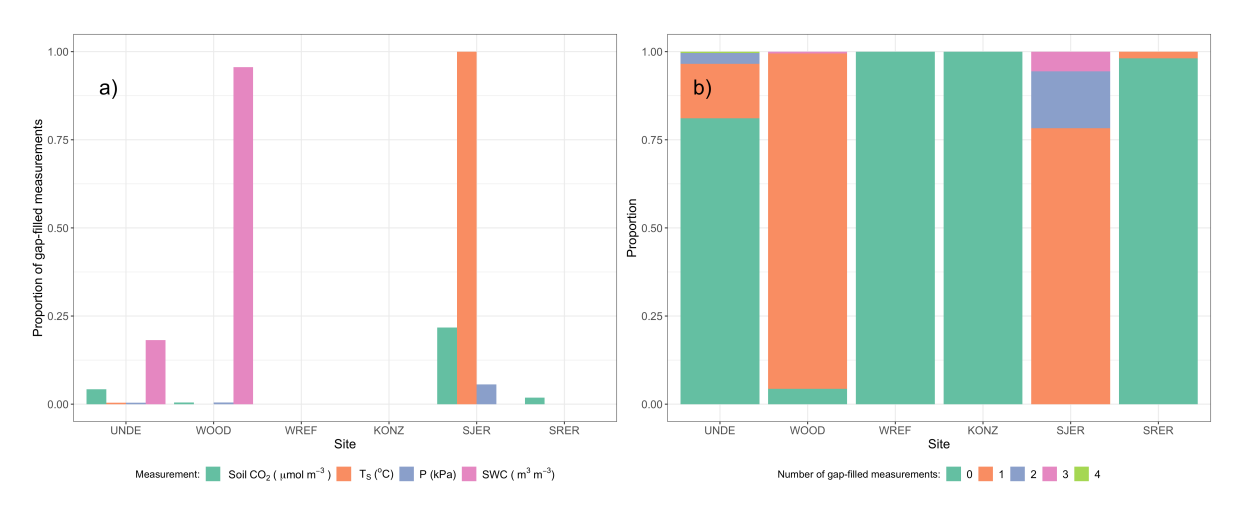


Figure S1: Panel a) Proportion of input gap-filled environmental measurements used to generate F_S from the neonSoilFlux package, by study site. Panel b) distribution of the usage of gap-filled measurements at each site.

2 Assessing the signal to noise ratio (SNR) and evaluating

estimated uncertainties

27

- Following collection of field measurements and calculation of the soil fluxes from neonSoilFlux
- $_{29}$ $\,$ package, we compared measured F_S based on closed-dynamic chamber measurements with the
- 30 LI-COR instruments to a given soil flux calculation from neonSoilFlux for each site and flux
- 31 computation method. Beyond the model statistics defined in the main text, we computed the
- signal to noise ratio (SNR), defined as the ratio of a modeled soil flux (F_{ijk}) from neonSoilFlux
- to its quadrature uncertainty (σ_{ijk}) .
- We observed that the range of values (e.g. $F_{ijk} \pm \sigma_{ijk}$ was much larger than the measured
- $_{\rm 35}$ $\,$ field flux. We evaluated $|F_S-F_{ijk}|<(1-\epsilon)\sigma_{ijk},$ where F_S is a measured field soil flux from
- the LI-COR 6800 (as the LI-COR 870/8250 was used at only three sites in 2024 but the 6800
- was used at all sites in both years). The parameter ϵ was an uncertainty reduction factor to
- evaluate how much the quadrature uncertainty could be reduced while maintaining precision
- between modeled F_{ijk} and measured F_S .
- 40 The computed signal to noise ratio (SNR) and the proportion of measured field fluxes within
- the modeled uncertainty for a given flux computation method F_{ijk} suggest that there was
- substantial variability in the agreement between the gradient method and field-measured ob-
- servations (Figure S2, Section 4.3 of the main text). Here, values of SNR greater than unity
- 44 indicate lower reported uncertainty, as propagated by quadrature due to a relatively higher
- precision of measured input variables (CO_2 , T_S , SWC, or P).
- The sensitivity to an uncertainty reduction factor (ϵ , bottom panels in Figure S2) demonstrates
- 47 how concordance between measured and modeled fluxes would be affected if environmental
- measurement uncertainty σ_{ijk} were to decrease. As ϵ increases from left to right in each figure,

- the possible range of values for each predicted flux value decreases and the proportion of
- 50 measured fluxes that fall within that range also decreases.

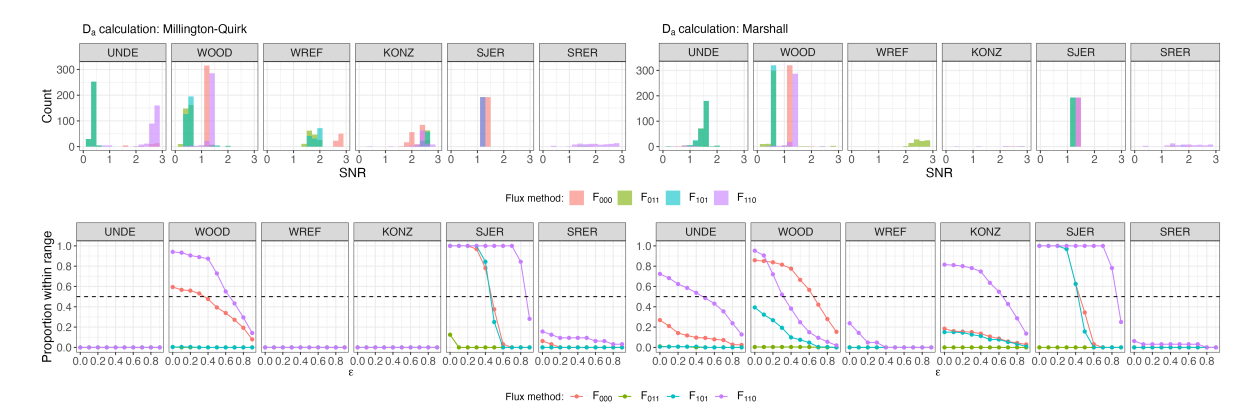


Figure S2: Top panels: distribution of SNR values across each of the different sites for modeled effluxes from the neonSoilFlux package, depending on the diffusivity calculation used (Millington-Quirk or Marshall, Section 4.2.2 of the main text). Bottom panels: Proportion of measured F_S within the modeled range of a flux computation method F_{ijk} given an uncertainty reduction factor ϵ , or $|F_S - F_{ijk}| < (1 - \epsilon)\sigma_{ijk}$.